

# ASSESSING FUTURE PROJECTIONS OF CLIMATE EXTREMES OVER THE SOUTH-CENTRAL UNITED STATES

Dana L. Gillson<sup>1</sup>, Esther Mullens<sup>2</sup>, Derek Rosendahl<sup>2</sup>

<sup>1</sup>National Weather Center Research Experiences for Undergraduates Program  
Norman, Oklahoma

<sup>2</sup>South Central Climate Science Center  
Norman, Oklahoma

## ABSTRACT

Climate extremes (heavy precipitation, drought, heat waves, storms, etc.) adversely affect numerous socioeconomic systems including infrastructure, economy, agriculture, and ecosystems. Understanding observed extremes events in the past and being able to determine how well climate models capture these will help planning and adaptation to climate stressors. The Expert Team on Climate Change and Detection (ETCCDI) have defined and developed a list of 27 core climate extreme indices that measure temperature and precipitation. Previous studies have compared the reliability of these extremes in a variety of regions but very few have done so with a focus on the south-central United States. This study uses 11 of the climate extreme indices to analyze climate extremes from historical observation-based reanalyses (ERA40, ERA-Interim, NCEP1, NCEP2) as well as historical and future projections of 31 global climate models (GCMs) from the Couple Model Intercomparison Project Phase 5 (CMIP5). We split the south-central region into three sub-regions (west-central, south-central and east-central). Results indicated that observation-based reanalyses can be significantly different from one another and therefore result in varying model biases depending on which reanalysis is used. Model performance is dependent on region, season, and extreme indices, and therefore no single model was found to be best for all situations. Similar models from the same institutions tend to contain similar biases within and across regions. This study also provides future projections that show a possible differentiation between the best and worst performing models.

---

## 1. INTRODUCTION

Climate extremes such as heavy precipitation, heat waves, drought, and storms adversely affects numerous socioeconomic and biological systems including infrastructure, economy, agriculture, and ecosystems, among others. The south-central region of the United States (US) experiences a variety of climate and

weather extremes that can damage and strain communities. This region is experiencing and will continue to experience loss of: water, land and energy security, ecosystem diversity, agricultural prosperity and sustainability, and human adaptability as a result of climate change (Shafer et al. 2014).

Climate models simulate various components of the earth system including

---

<sup>1</sup> *Corresponding author address:* Dana Gillson,  
Mount Holyoke College, E-mail:  
gills22d@mtholyoke.edu

the atmosphere, ocean, biosphere, and cryosphere, among others. These models simulate historical and future climate conditions. Historical simulations, when compared with observed past conditions, can help researchers to better understand the uncertainty of future climate projections. Observational reanalyses reconstruct past climate, therefore, giving us a means of comparison or “ground truth” to compare with projected climate extremes. This allows researchers to examine extreme aspects of climate, including temperature and precipitation.

While observational reanalyses can be used to evaluate climate model historical projections, research has shown discrepancies between different historical reanalyses, suggesting that there are inconsistencies in their ability to represent past extremes (Sillmann et al. 2013). Validating the variability of climate extremes simulated by climate models is essential in order to better understand whether models represent the overall frequency and variability of extreme temperatures, and precipitation. In addition, determining the degree of variability in model to observation differences when applying different reanalysis products can help researchers understand the degree to which different ‘ground truths’ can impact their results. With this understanding we are able to anticipate and plan for extremes in the future on a global and local scale. Increased understanding of how climate extremes may fluctuate in the future will benefit stakeholders and decision makers impacted by these changes. In order to address the problem, this work will use a suite of metrics for extremes in temperature and precipitation, obtained from the Expert Team on Climate Change and Detection Indices (ETCCDI, Alexander et al. 2006).

Our research addresses three primary goals. Firstly, to examine the range of historical climate extreme events in the south-central U.S. using reanalysis datasets. Secondly, to explore how well climate models capture the range of these events by comparing reanalysis datasets to GCM historical simulations and determining model biases. Lastly, we analyze how these biases effect the way future extreme events are projected, and how these climate extreme events might change in the future.

## 2. DATA AND METHODS

### *Study Area*

We focused on the south-central region of the U.S. and divided it into three regions (i.e. west-central, south-central, and east-central). Figure 1 shows the regional domains.

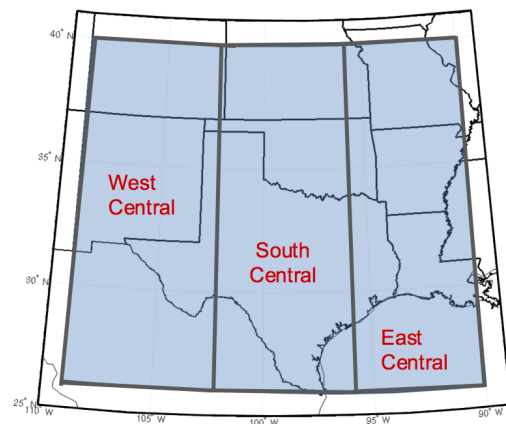


**Figure 1:** Region for analysis split into three sub-regions of focus.

The region was split into three sub-regions in order to more accurately reflect the climate extremes across the precipitation gradient in the south-central U.S. (Figure 2). The east-central portion is generally more humid and closer to sea-level which contrasts significantly with the semi-arid and mountainous terrain of the west-central. The south-central sub-region consists of

relatively flat grasslands. Variation in climate change impacts are likely due to the apparent diversity within the region (Shafer et al. 2014).

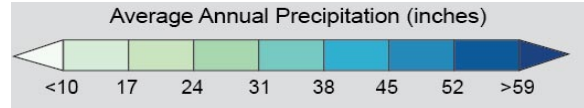
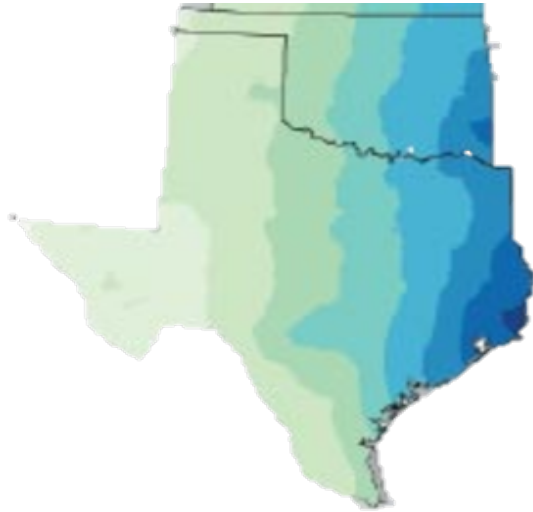


**Figure 2 (left):** Precipitation gradient across Oklahoma and Texas. (Adapted from Kunkel 2013)

*Data*

ETCCDI defined a list of 27 core climate extreme indices of temperature and precipitation (Alexander et al. 2006). These indices offer additional information on extremes in climate that general mean values cannot provide. The climate extreme indices were obtained from the ETCCDI indices archived at <http://www.cccma.ec.gc.ca/data/climdex/>. We investigated 11 out of the 27 defined indices (see Table 1).

Index Names & Descriptions	Index Abbreviation
Percentage of Cold Nights (below 10 <sup>th</sup> percentile)	TN10p
Percentage of Cold Days (below 10 <sup>th</sup> percentile)	TX10p
Percentage of Warm Nights (above 90 <sup>th</sup> percentile)	TN90p
Percentage of Warm Days (above 90 <sup>th</sup> percentile)	TX90p
Max. 1 day precipitation	RX1day
Max 5 day precipitation	RX5day
Max. daily max. temp. per month	TXx
Min. daily max. temp. per month	TXn
Max. daily min. temp. per month	TNx
Min. daily min. temp per month	TNn
Diurnal temp. range- difference in daily max and min temp.	DTR

**Table 1:** The 11 extreme indices used for this project, defined by the ETCCDI.

The Climate extreme indices used in this study have been calculated for the majority of global climate models (GCMs) from the Coupled Model Intercomparison project Phase 5 (CMIP5). The CMIP5 GCMs improve upon previous climate models by including interactive ocean and carbon cycles, the indirect effect of aerosols, and (in some models) the projection of volcanic and solar forcing (Sillmann et al. 2013). CMIP5 provides historical simulations and future projections out to 2100 (<http://cmip-pcmdi.llnl.gov/cmip5/>). Extremes indices are also available from four reanalyses datasets. Reanalyses are model simulations that are driven by observational data. Reanalyses have a gridded output similar to that of GCMs. This allows them to be easily compared to model simulations (Sillmann et al. 2013). We utilized four reanalyses: ERA40, ERAInterim, National Center for Environmental Prediction/National Center for Atmospheric Research (NCEP/NCAR) Reanalysis 1 (NCEP1), and NCEP-DOE Reanalysis 2 (NCEP2).

### *Methodology*

We used 30 of the 38 available CMIP5 model datasets, and 11 extremes indices. These datasets had both historical and future model output that were regridded (into a 2x2 degree grid) over our sub-domains using an NCAR Command Line (NCL) program, which converted NetCDF to text files. A similar NCL program was used in order to output text files for the four reanalyses across the three sub-regions. All of the reanalyses are created using different methods and span different time periods meaning that their computed historical data can differ from one another. For each reanalysis dataset, all available years in the data were included. The historical period was typically 1850-2005. The CMIP5 future period was typically from 2006 to 2100. We

used this time period when projecting extremes into the future. Three emission representative concentration pathways (RCPs; Friedlingstein et al. 2014) were considered: RCP2.6, 4.5, and 8.5. RCPs are emissions scenarios calculated based on projections of anthropogenic greenhouse gas emissions. RCP2.6 projects relatively small amounts of anthropogenic greenhouse gas emissions while RCP8.5 represents continuously high greenhouse gas emissions. In most cases, we used only the first available ensemble member, for which the extremes had already been calculated.

In order to better understand how each GCM extreme diverges from reanalysis in the historical period, we calculated a seasonal percentage bias for each of the 11 extreme indices. Another NCL program was created to calculate these biases. The percentage bias of each GCM is relative to each reanalysis, and the climatology used to extract percentage bias was the length of the reanalysis dataset. The seasonal percentage biases for each of the 11 extreme indices were calculated for each model by comparing its historical data against the four reanalysis data sets. The percentage biases were averaged over all seasons and GCMs. The mean percentage bias was also calculated for each region by averaging the biases obtained from using the four different 'ground truth' reanalyses. All of these calculations were used in order to create a bias (portrait) diagram for each region. Bias/portrait diagrams displays the mean percentage bias per season across each model and extreme, and was adapted from Sillmann et al. (2013).

The next step was the calculation of the absolute value for the bias percentage for all the extremes for each season per region. The mean of each season was averaged to get the all season average (per model). We used

these cumulative percentage biases to rank the models in order by performance. The five best and worst models over all seasons for the south-central subdomain were used to assess modeled future projections. Due to time constraints, we assessed future trends for only three select extremes: maximum 5-day precipitation, percentage of cold days below the 10<sup>th</sup> percentile, and percentage of warm days above the 90<sup>th</sup> percentile (respectively: RX5days, TN10p, and TX90p). These three extremes represent a glimpse of overall precipitation and temperature events and trends. Only RCP8.5 was assessed because it offers the greatest growth in emission, and thus, the largest anthropogenic climate change signal. We used data from all four of the reanalyses in order to represent the historical period.

### 3. RESULTS

Tables 2, 3, and 4 show the bias/portrait diagrams that were created for each sub-region. The colors in the diagram represent the percentage bias with warm colors showing a higher bias than cooler colors. Dashes (-) inside the box indicate that the model has a negative (cold/dry) bias, while an empty box indicates a positive (warm/wet) bias. In general, biases for most of the extreme indices examined were more pronounced during the spring or fall months for each region. Larger model vs reanalysis biases are also evident in summer in the westernmost sub-domain (Table 4) for maximum one day and maximum 5-day precipitation (RX1day and RX5 day respectively) in the west-central region (Table 4). These extremes show a

particularly high bias in comparison to the south- and east-central regions.

Across the entire south-central U.S., minimum daily temperature (TNn) has a high bias independent of the model, typically exceeding 80% or even 100%. Although, you can see a noticeably higher bias in all three regions, it seems to particularly impact the south- and west-central domains. With this variable in particular, we identified that some reanalysis data (particularly NCEP1) was close to 0°C when averaged seasonally. Compared model values would therefore create a very large percentage bias (up to 539% in this case) if they were not also close to 0. Failing to normalize the percentage biases presented itself as a limitation within this study. We could also have converted temperature data to Kelvins rather than degrees Celsius.

The comparison of the absolute values of the percentage biases for each observation-based reanalysis is shown in Table 5. The significantly larger biases of TNn are numerically exemplified across each region and reanalysis. Additionally, you can see that a higher bias is calculated for RX1day and RX5day in the west-central compared to the other two regions. The GCMs bias relative to ERA40 for these extremes in the west-central region are substantially larger than other regions or reanalyses. In each region the CMIP5 data that best agrees with a given reanalysis differs. Table 6 shows the average of each reanalysis across all of the extreme indices and the 3 domains. It shows that the GCMs are least biased when ERAInterim is the observation, which can also be seen in the values in Table 5.

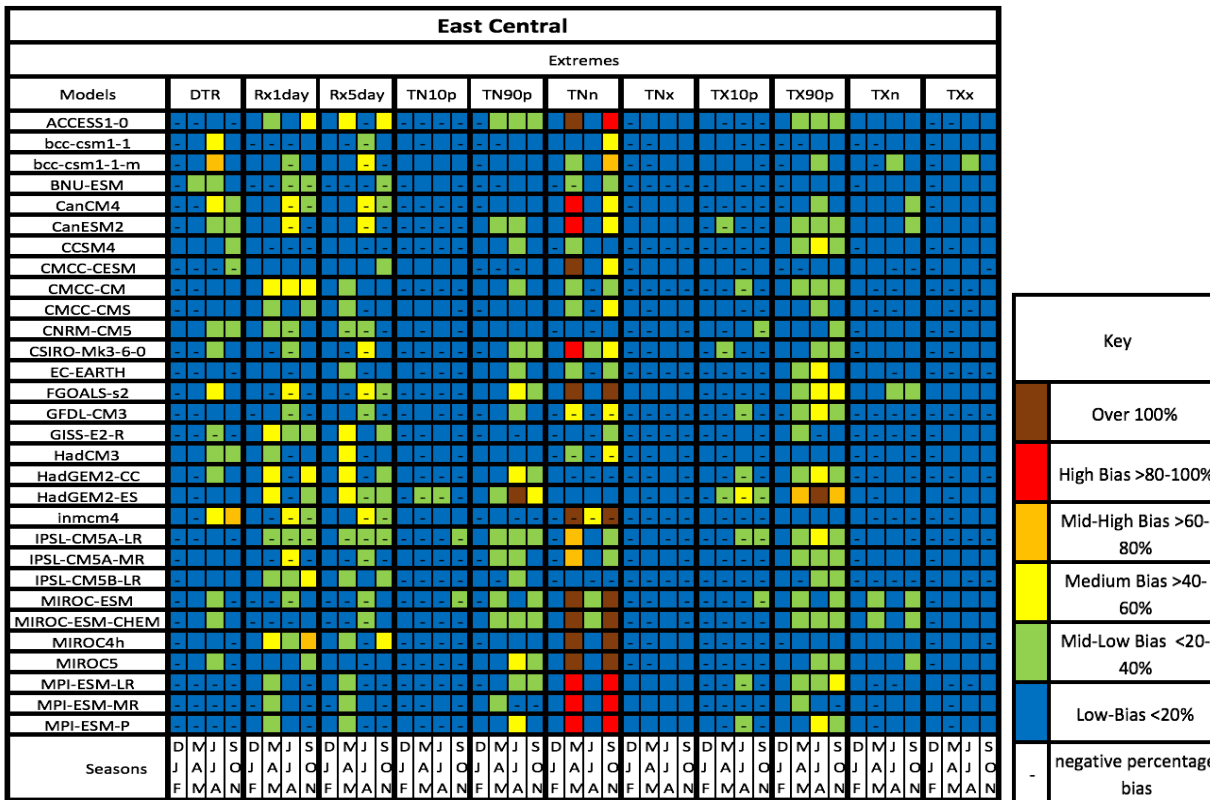


**Table 2:** East-central bias/portrait diagram demonstrating the percentage bias for each of the 11 selected extremes across all 30 GCMs. Negative percentage biases are shown as dashed within a corresponding box.

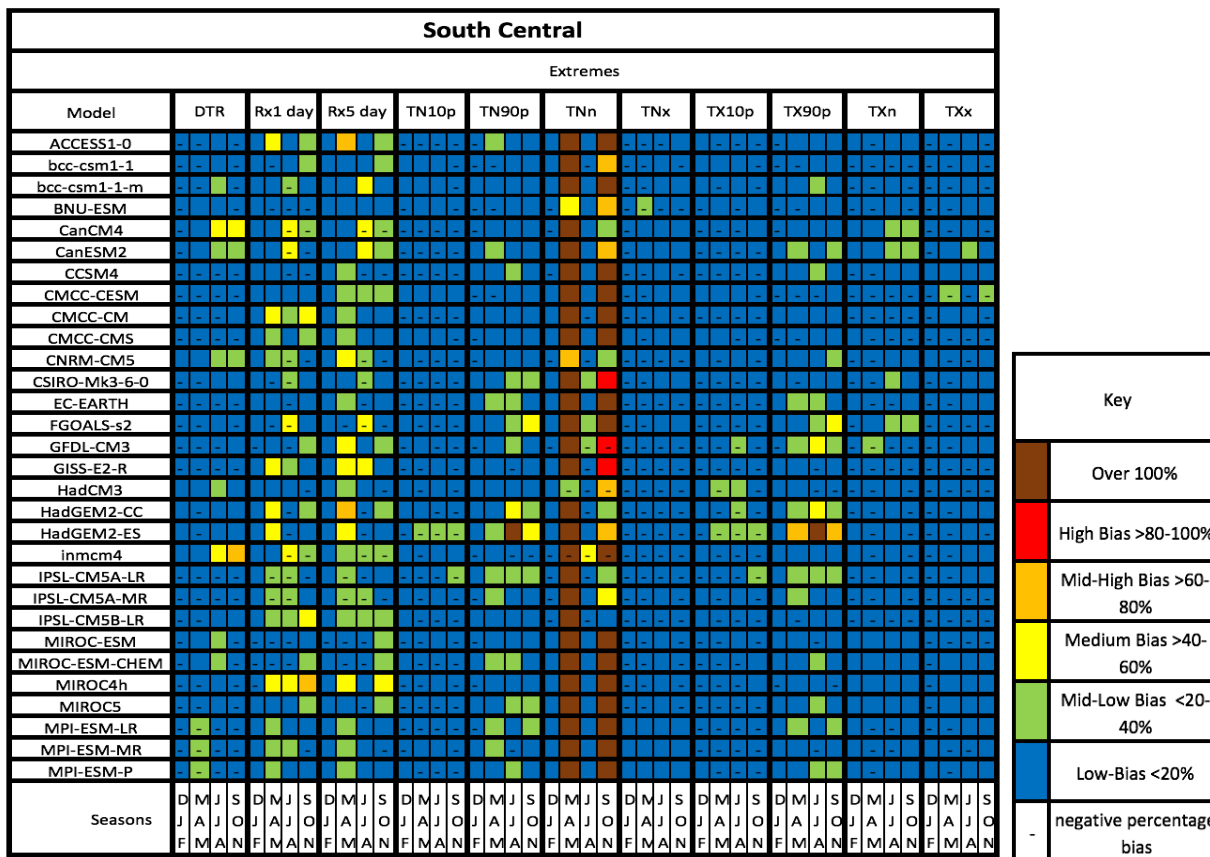


**Table 3:** Same as Table 2 but for the south-central region.

West Central												
Extremes												
Model	DTR	Rx1day	Rx5day	TN10p	TN90p	TNn	TNx	TX10p	TX90p	TXn	TXx	
ACCESS1-0												
bcc-csm1-1												
bcc-csm1-1-m												
BNU-ESM												
CanCM4												
CanESM2												
CCSM4												
CMCC-CE5M												
CMCC-CM												
CMCC-CMS												
CNRM-CM5												
CSIRO-Mk3-6-0												
EC-EARTH												
FGOALS-s2												
GFDL-CM3												
GISS-E2-R												
HadCM3												
HadGEM2-CC												
HadGEM2-ES												
inmcm4												
IPSL-CM5A-LR												
IPSL-CM5A-MR												
IPSL-CM5B-LR												
MIROC-ESM												
MIROC-ESM-CHEM												
MIROC4h												
MIROC5												
MPI-ESM-LR												
MPI-ESM-MR												
MPI-ESM-P												
Seasons	D M J J A J F M A	S O J A J N F M	D M J J A J F M A	S O J A J N F M	D M J J A J F M A	S O J A J N F M	D M J J A J F M A	S O J A J N F M	D M J J A J F M A	S O J A J N F M	D M J J A J F M A	S O J A J N F M

Key

- Over 100%
- High Bias >80-100%
- Mid-High Bias >60-80%
- Medium Bias >40-60%
- Mid-Low Bias <20-40%
- Low-Bias <20%
- negative percentage bias

Table 4: Same as Table 2 but for the west-central region.

Regions	East Central				South Central				West Central			
	Bias ERA40	Bias ERAInterim	Bias NCEP1	Bias NCEP2	Bias ERA40	Bias ERAInterim	Bias NCEP1	Bias NCEP2	Bias ERA40	Bias ERAInterim	Bias NCEP1	Bias NCEP2
DTR	15.79	11.96	10.40	10.29	13.90	10.49	13.73	9.68	11.21	10.31	16.18	10.59
RX1day	31.01	15.41	18.17	20.51	33.51	13.88	18.53	19.63	44.96	19.26	34.59	17.69
Rx5day	29.24	13.70	17.39	19.97	38.36	13.48	13.81	18.37	58.11	22.41	35.10	19.98
TN10p	4.59	12.28	6.03	11.69	3.94	10.99	6.02	10.39	3.52	12.22	6.15	12.08
TN90p	5.84	21.06	5.67	20.88	4.99	18.86	5.37	17.36	3.24	19.37	4.86	17.46
TNn	21.45	21.20	53.19	64.88	27.04	26.80	539.63	160.04	189.10	131.58	54.56	54.89
TNx	2.98	2.82	3.24	2.86	3.86	3.44	3.69	4.45	7.66	6.35	6.50	7.96
TX10p	5.82	15.58	4.60	14.51	3.94	10.27	4.03	9.56	3.18	10.94	5.95	10.11
TX90p	10.37	23.24	8.66	20.78	5.92	19.58	4.93	15.75	4.19	22.87	9.15	20.14
TXn	6.36	5.27	5.16	5.77	6.37	6.05	6.74	5.93	7.22	8.03	9.15	7.14
TXx	4.77	4.20	3.68	3.52	4.18	3.66	4.31	3.61	4.65	4.59	8.56	4.92
<b>Averages</b>	<b>12.57</b>	<b>13.34</b>	<b>12.38</b>	<b>17.79</b>	<b>13.27</b>	<b>12.50</b>	<b>56.44</b>	<b>24.98</b>	<b>30.64</b>	<b>24.36</b>	<b>17.34</b>	<b>16.63</b>

Table 5: Comparison of the absolute values of the extreme indices percentage biases for each observation-based reanalysis.

Bias ERA40	Bias ERAInterim	Bias NCEP1	Bias NCEP2
18.83	16.73	28.72	19.80

Table 6: Average of each absolute value percentage bias across all of the extreme indices and the three domains.

East Central									
Model	All Seasons Average	Model	Winter Average	Model	Spring Average	Model	Summer Average	Model	Fall Average
BNU-ESM	0.22	MIROC-ESM-	0.03	bcc-csm1-1	0.02	EC-EARTH	0.11	BNU-ESM	0.46
IPSL-CM5A-LR	0.48	CSIRO-Mk3-6-0	0.04	BNU-ESM	2.5	IPSL-CM5A-MR	0.12	HadCM3	1.66
HadCM3	2	CNRM-CM5	0.04	GFDL-CM3	2.76	CMCC-CESM	0.41	IPSL-CM5A-LR	2
IPSL-CM5A-MR	2.6	CCSM4	0.04	CSIRO-Mk3-6-0	4.17	GISS-E2-R	0.54	IPSL-CM5A-MR	3.06
EC-EARTH	3.04	MIROC4h	0.05	HadCM3	4.23	IPSL-CM5A-LR	0.78	GFDL-CM3	3.36
CNRM-CM5	3.15	MIROC-ESM	0.07	IPSL-CM5A-LR	4.56	CNRM-CM5	1.1	CCSM4	4.31
GFDL-CM3	3.29	inmcm4	0.07	IPSL-CM5B-LR	5.04	MPI-ESM-MR	1.11	CNRM-CM5	4.35
bcc-csm1-1	3.43	MPI-ESM-MR	0.1	bcc-csm1-1-m	5.36	CanCM4	2.01	EC-EARTH	4.46
GISS-E2-R	3.86	bcc-csm1-1	0.1	CCSM4	6.63	CanESM2	2.19	GISS-E2-R	5.24
CCSM4	3.96	CanCM4	0.11	CNRM-CM5	7.11	MPI-ESM-LR	2.52	IPSL-CM5B-LR	6.2
IPSL-CM5B-LR	4.27	bcc-csm1-1-m	0.12	IPSL-CM5A-MR	7.2	BNU-ESM	3.38	MPI-ESM-MR	6.71
CSIRO-Mk3-6-0	4.3	IPSL-CM5A-LR	0.12	EC-EARTH	7.54	MIROC-ESM	4.108	CSIRO-Mk3-6-0	7.29
CMCC-CESM	5.33	IPSL-CM5B-LR	0.13	CMCC-CMS	9.21	CMCC-CMS	4.19	CMCC-CMS	7.6
CMCC-CMS	5.34	FGOALS-s2	0.14	HadGEM2-CC	9.63	ACCESS1-0	4.2	bcc-csm1-1	7.85
MPI-ESM-MR	5.57	GISS-E2-R	0.14	MPI-ESM-P	10	MIROC-ESM-	4.59	CanESM2	8.26
CanCM4	5.76	MIROC5	0.18	CMCC-CM	10.01	inmcm4	4.72	CanCM4	8.88
HadGEM2-CC	6.13	HadCM3	0.22	GISS-E2-R	10.59	CCSM4	4.88	CMCC-CESM	8.91
bcc-csm1-1-m	6.61	MPI-ESM-LR	0.23	CMCC-CESM	11.72	HadGEM2-CC	4.94	HadGEM2-CC	9.46
MPI-ESM-LR	6.88	IPSL-CM5A-MR	0.24	CanCM4	12.035	HadCM3	5.19	CMCC-CM	11.37
CanESM2	6.95	MPI-ESM-P	0.28	MPI-ESM-LR	12.52	CSIRO-Mk3-6-0	5.71	MPI-ESM-P	11.66
CMCC-CM	7.27	EC-EARTH	0.29	inmcm4	13.39	IPSL-CM5B-LR	5.71	MPI-ESM-LR	12.27
MPI-ESM-P	7.31	CMCC-CESM	0.29	MPI-ESM-MR	14.35	GFDL-CM3	5.93	bcc-csm1-1-m	13.12
inmcm4	9.99	CanESM2	0.36	HadGEM2-ES	14.97	bcc-csm1-1	5.97	HadGEM2-ES	15.36
FGOALS-s2	10.38	CMCC-CMS	0.37	FGOALS-s2	15.62	FGOALS-s2	5.98	MIROC-ESM	17.33
MIROC-ESM	10.88	CMCC-CM	0.44	CanESM2	17	CMCC-CM	7.25	MIROC-ESM-	19.37
ACCESS1-0	11.57	BNU-ESM	0.47	MIROC5	17.2	MPI-ESM-P	7.29	ACCESS1-0	19.61
MIROC5	11.91	HadGEM2-CC	0.47	ACCESS1-0	21.96	MIROC4h	7.45	FGOALS-s2	19.78
MIROC-ESM-	11.97	ACCESS1-0	0.5	MIROC-ESM	22.15	bcc-csm1-1-m	7.86	MIROC5	20.01
HadGEM2-ES	12.01	HadGEM2-ES	0.65	MIROC4h	23.53	MIROC5	10.25	inmcm4	21.92
MIROC4h	13.94	GFDL-CM3	1.1	MIROC-ESM-	23.89	HadGEM2-ES	17.07	MIROC4h	24.84

**Table 7:** Ranking of the GCMs for the east-central region by averaging the extremes indices percentage biases across all seasons as well as per season. The percentage biases highlighted in green are those with lowest bias (the “best” models), while the ones highlighted in red are the highest percentage biases (the “worst” models).

South Central									
Model	All Seasons Average	Model	Winter Average	Model	Spring Average	Model	Summer Average	Model	Fall Average
HadCM3	0.69	MIROC-ESM	0.008	HadCM3	0.23	EC-EARTH	0.19	IPSL-CM5A-LR	0.39
GFDL-CM3	1.71	GISS-E2-R	0.01	BNU-ESM	2.4	CNRM-CM5	0.24	GFDL-CM3	3.88
BNU-ESM	3.41	CNRM-CM5	0.03	CNRM-CM5	12.23	FGOALS-s2	0.63	IPSL-CM5A-MR	4.53
CNRM-CM5	4.46	IPSL-CM5A-MR	0.05	GFDL-CM3	13.73	IPSL-CM5A-LR	0.99	CanCM4	4.65
IPSL-CM5B-LR	7.21	CanCM4	0.06	IPSL-CM5B-LR	20.87	IPSL-CM5B-LR	1.54	CNRM-CM5	5.33
IPSL-CM5A-LR	7.85	CCSM4	0.08	HadGEM2-CC	27.58	CMCC-CESM	1.72	IPSL-CM5B-LR	6.28
IPSL-CM5A-MR	9.36	MIROC-ESM-CHEM	0.08	bcc-csm1-1	28.94	CanCM4	1.98	BNU-ESM	6.75
CanCM4	11.06	EC-EARTH	0.09	IPSL-CM5A-LR	31.87	GFDL-CM3	2.16	HadCM3	7.91
HadGEM2-CC	11.14	HadCM3	0.11	IPSL-CM5A-MR	35.48	MPI-ESM-LR	2.29	CanESM2	9.07
bcc-csm1-1	11.43	CSIRO-Mk3-6-0	0.12	CanCM4	37.68	MPI-ESM-MR	2.3	GISS-E2-R	10.21
GISS-E2-R	13.52	MIROC5	0.13	bcc-csm1-1-m	40.28	IPSL-CM5A-MR	2.61	bcc-csm1-1	10.44
EC-EARTH	13.74	IPSL-CM5B-LR	0.14	HadGEM2-ES	40.93	GISS-E2-R	2.81	HadGEM2-CC	10.47
CanESM2	14.89	ACCESS1-0	0.14	GISS-E2-R	41.06	bcc-csm1-1-m	2.89	CSIRO-Mk3-6-0	10.83
bcc-csm1-1-m	15.12	IPSL-CM5A-LR	0.15	EC-EARTH	43.72	CanESM2	3.27	EC-EARTH	11.35
HadGEM2-ES	17.76	MPI-ESM-MR	0.15	CanESM2	46.98	CSIRO-Mk3-6-0	3.27	CMCC-CESM	12.68
CSIRO-Mk3-6-0	18.23	bcc-csm1-1-m	0.15	CCSM4	53.57	MIROC-ESM	3.31	bcc-csm1-1-m	15.12
CCSM4	18.65	CMCC-CESM	0.16	CSIRO-Mk3-6-0	58.7	CMCC-CM	3.53	HadGEM2-ES	15.26
CMCC-CM	20.99	bcc-csm1-1	0.18	CMCC-CM	64.15	CMCC-CMS	3.73	CCSM4	15.34
CMCC-CESM	22.13	MPI-ESM-LR	0.2	CMCC-CMS	72.07	MPI-ESM-P	4.32	MPI-ESM-MR	15.74
CMCC-CMS	23.02	MIROC4h	0.2	CMCC-CESM	73.94	BNU-ESM	4.71	CMCC-CMS	15.92
MPI-ESM-MR	24.32	inmcm4	0.22	MPI-ESM-MR	79.1	ACCESS1-0	5.16	CMCC-CM	15.96
MPI-ESM-LR	25.93	HadGEM2-CC	0.22	MPI-ESM-LR	81.01	HadCM3	5.26	MPI-ESM-LR	20.22
MPI-ESM-P	27.34	CanESM2	0.23	MPI-ESM-P	81.74	CCSM4	5.62	MPI-ESM-P	23.08
ACCESS1-0	27.85	BNU-ESM	0.23	ACCESS1-0	82.42	bcc-csm1-1	6.17	ACCESS1-0	23.68
MIROC-ESM	28.37	MPI-ESM-P	0.23	MIROC-ESM	85.81	MIROC-ESM-CHEM	6.17	MIROC-ESM	24.36
FGOALS-s2	30.69	HadGEM2-ES	0.3	inmcm4	86.17	inmcm4	6.19	MIROC-ESM-CHEM	26.85
MIROC-ESM-CHEM	30.99	FGOALS-s2	0.31	FGOALS-s2	86.57	HadGEM2-CC	6.29	MIROC5	33.87
MIROC5	33.83	CMCC-CMS	0.33	MIROC-ESM-CHEM	90.85	MIROC5	8.18	FGOALS-s2	35.26
inmcm4	34.27	CMCC-CMS	0.36	MIROC5	93.13	MIROC4h	12.58	MIROC4h	36.01
MIROC4h	39.11	GFDL-CM3	0.85	MIROC4h	108.05	HadGEM2-ES	14.57	inmcm4	44.92

Table 8: Same as Table 7 but for south-central region.

West Central									
Model	All Seasons Average	Model	Winter Average	Model	Spring Average	Model	Summer Average	Model	Fall Average
CMCC-CESM	0.27	CSIRO-Mk3-6-0	0.001	CMCC-CMS	0.47	CanESM2	0.26	BNU-ESM	0.38
CMCC-CM	0.63	CanESM2	0.003	MPI-ESM-MR	1.73	GFDL-CM3	0.46	GISS-E2-R	0.93
EC-EARTH	0.94	EC-EARTH	0.01	MPI-ESM-LR	2.68	CMCC-CM	1.51	bcc-csm1-1	1.09
HadCM3	1.06	CNRM-CM5	0.03	CMCC-CM	3	CanCM4	1.68	CMCC-CM	2.35
CSIRO-Mk3-6-0	1.29	ACCESS1-0	0.03	MIROC4h	3.84	EC-EARTH	2.2	MPI-ESM-MR	2.57
GFDL-CM3	1.5	IPSL-CM5A-MR	0.04	IPSL-CM5A-LR	4.46	HadCM3	2.67	bcc-csm1-1-m	2.96
IPSL-CM5A-MR	1.88	MIROC-ESM	0.08	CCSM4	5.73	bcc-csm1-1-m	3.27	ACCESS1-0	3.03
MPI-ESM-P	1.92	MIROC5	0.08	CSIRO-Mk3-6-0	6.18	CNRM-CM5	3.32	MPI-ESM-LR	3.29
CMCC-CMS	2	MIROC-ESM-	0.09	IPSL-CM5A-MR	6.57	IPSL-CM5B-LR	3.58	CMCC-CMS	3.37
ACCESS1-0	2.05	IPSL-CM5A-LR	0.1	ACCESS1-0	7.23	ACCESS1-0	3.99	CCSM4	3.68
MPI-ESM-LR	2.06	CCSM4	0.12	MIROC-ESM-	7.25	CMCC-CMS	4.73	CMCC-CESM	4.26
IPSL-CM5B-LR	2.15	CanCM4	0.15	MPI-ESM-P	8.24	IPSL-CM5A-MR	4.78	IPSL-CM5B-LR	4.8
MPI-ESM-MR	2.59	inmcm4	0.16	MIROC-ESM	8.79	CSIRO-Mk3-6-0	4.94	HadGEM2-ES	4.98
IPSL-CM5A-LR	3.73	bcc-csm1-1-m	0.2	MIROC5	9.18	bcc-csm1-1	4.95	MPI-ESM-P	8.42
bcc-csm1-1	3.84	HadCM3	0.21	bcc-csm1-1	11.27	FGOALS-s2	5.31	IPSL-CM5A-MR	9.36
CanESM2	3.98	HadGEM2-CC	0.21	CMCC-CESM	11.83	MPI-ESM-MR	5.74	GFDL-CM3	9.88
CanCM4	4.2	bcc-csm1-1	0.22	FGOALS-s2	15.43	CMCC-CESM	6.21	HadGEM2-CC	10.08
MIROC-ESM	4.8	HadGEM2-ES	0.23	GFDL-CM3	16.55	GISS-E2-R	6.5	MIROC4h	11.7
MIROC5	5.12	MPI-ESM-LR	0.23	IPSL-CM5B-LR	16.64	IPSL-CM5A-LR	6.59	EC-EARTH	12.09
bcc-csm1-1-m	5.16	GISS-E2-R	0.26	EC-EARTH	18.02	MPI-ESM-P	7.23	IPSL-CM5A-LR	12.87
FGOALS-s2	5.32	MPI-ESM-P	0.26	HadGEM2-ES	20.09	MPI-ESM-LR	7.4	CNRM-CM5	13.82
CCSM4	5.35	CMCC-CESM	0.28	bcc-csm1-1-m	20.14	HadGEM2-CC	9.43	CanESM2	14.83
HadGEM2-CC	5.65	MIROC4h	0.28	BNU-ESM	20.53	inmcm4	9.65	MIROC-ESM	15.16
inmcm4	5.82	BNU-ESM	0.29	GISS-E2-R	21.18	BNU-ESM	10.12	MIROC5	15.2
MIROC-ESM-	6.19	MPI-ESM-MR	0.31	HadGEM2-CC	23.03	CCSM4	11.85	CSIRO-Mk3-6-0	16.29
GISS-E2-R	6.75	IPSL-CM5B-LR	0.33	HadCM3	25.65	MIROC-ESM	12.77	CanCM4	17.96
HadGEM2-ES	7.06	FGOALS-s2	0.36	CanESM2	30.48	HadGEM2-ES	12.91	MIROC-ESM-	11.32
BNU-ESM	7.5	CMCC-CM	0.36	CanCM4	36.6	MIROC-ESM-	13.61	HadCM3	24.28
MIROC4h	9.8	CMCC-CMS	0.39	CNRM-CM5	50.51	MIROC5	14.39	FGOALS-s2	31.03
CNRM-CM5	10.01	GFDL-CM3	1.14	inmcm4	87.36	MIROC4h	23.93	inmcm4	54.59

Table 9: Same as Table 7 but for west-central region.

	Model	All Seasons Average	Model	Winter Average	Model	Spring Average	Model	Summer Average	Model	Fall Average
East-Central	BNU-ESM	0.22	MIROC-ESM-CHEM	0.03	bcc-csm1-1	0.02	EC-EARTH	0.11	BNU-ESM	0.46
	IPSL-CM5A-LR	0.48	CSIRO-Mk3-6-0	0.04	BNU-ESM	2.5	IPSL-CM5A-MR	0.12	HadCM3	1.66
	HadCM3	2	CNRM-CM5	0.04	GFDL-CM3	2.76	CMCC-CESM	0.41	IPSL-CM5A-LR	2
	IPSL-CM5A-MR	2.6	CCSM4	0.04	CSIRO-Mk3-6-0	4.17	GISS-E2-R	0.54	IPSL-CM5A-MR	3.06
	EC-EARTH	3.04	MIROC4h	0.05	HadCM3	4.23	IPSL-CM5A-LR	0.78	GFDL-CM3	3.36
	ACCESS1-0	11.57	BNU-ESM	0.47	MIROC5	17.2	MPI-ESM-P	7.29	ACCESS1-0	19.61
	MIROC5	11.91	HadGEM2-CC	0.47	ACCESS1-0	21.96	MIROC4h	7.45	FGOALS-s2	19.78
	MIROC-ESM-CHEM	11.97	ACCESS1-0	0.5	MIROC-ESM	22.15	bcc-csm1-1-m	7.86	MIROC5	20.01
	HadGEM2-ES	12.01	HadGEM2-ES	0.65	MIROC4h	23.53	MIROC5	10.25	inmcm4	21.92
	MIROC4h	13.94	GFDL-CM3	1.1	MIROC-ESM-CHEM	23.89	HadGEM2-ES	17.07	MIROC4h	24.84
South-Central	HadCM3	0.69	MIROC-ESM	0.008	HadCM3	0.23	EC-EARTH	0.19	IPSL-CM5A-LR	0.39
	GFDL-CM3	1.71	GISS-E2-R	0.01	BNU-ESM	2.4	CNRM-CM5	0.24	GFDL-CM3	3.88
	BNU-ESM	3.41	CNRM-CM5	0.03	CNRM-CM5	12.23	FGOALS-s2	0.63	IPSL-CM5A-MR	4.53
	CNRM-CM5	4.46	IPSL-CM5A-MR	0.05	GFDL-CM3	13.73	IPSL-CM5A-LR	0.99	CanCM4	4.65
	IPSL-CM5B-LR	7.21	CanCM4	0.06	IPSL-CM5B-LR	20.87	IPSL-CM5B-LR	1.54	CNRM-CM5	5.33
	FGOALS-s2	30.69	HadGEM2-ES	0.3	inmcm4	86.17	inmcm4	6.19	MIROC-ESM-CHEM	26.85
	MIROC-ESM-CHEM	30.99	FGOALS-s2	0.31	FGOALS-s2	86.57	HadGEM2-CC	6.29	MIROC5	33.87
	MIROC5	33.83	CMCC-CM	0.33	MIROC-ESM-CHEM	90.85	MIROC5	8.18	FGOALS-s2	35.26
	inmcm4	34.27	CMCC-CMS	0.36	MIROC5	93.13	MIROC4h	12.58	MIROC4h	36.01
	MIROC4h	39.11	GFDL-CM3	0.85	MIROC4h	108.05	HadGEM2-ES	14.57	inmcm4	44.92
West-Central	CMCC-CESM	0.27	CSIRO-Mk3-6-0	0.001	CMCC-CMS	0.47	CanESM2	0.26	BNU-ESM	0.38
	CMCC-CM	0.63	CanESM2	0.003	MPI-ESM-MR	1.73	GFDL-CM3	0.46	GISS-E2-R	0.93
	EC-EARTH	0.94	EC-EARTH	0.01	MPI-ESM-LR	2.68	CMCC-CM	1.51	bcc-csm1-1	1.09
	HadCM3	1.06	CNRM-CM5	0.03	CMCC-CM	3	CanCM4	1.68	CMCC-CM	2.35
	CSIRO-Mk3-6-0	1.29	ACCESS1-0	0.03	MIROC4h	3.84	EC-EARTH	2.2	MPI-ESM-MR	2.57
	GISS-E2-R	6.75	IPSL-CM5B-LR	0.33	HadCM3	25.65	MIROC-ESM	12.77	CanCM4	17.96
	HadGEM2-ES	7.06	FGOALS-s2	0.36	CanESM2	30.48	HadGEM2-ES	12.91	MIROC-ESM-CHEM	18.32
	BNU-ESM	7.5	CMCC-CM	0.36	CanCM4	36.6	MIROC-ESM-CHEM	13.61	HadCM3	24.28
	MIROC4h	9.8	CMCC-CMS	0.39	CNRM-CM5	50.51	MIROC5	14.39	FGOALS-s2	31.03
	CNRM-CM5	10.01	GFDL-CM3	1.14	inmcm4	87.36	MIROC4h	23.93	inmcm4	54.59

Table 10: Model name and percentage bias for the top and bottom GCMs per region for each seasonal group. The percentage biases highlighted in green are those with lowest bias (the “best” models), while the ones highlighted in red are the highest percentage biases (the “worst” models).

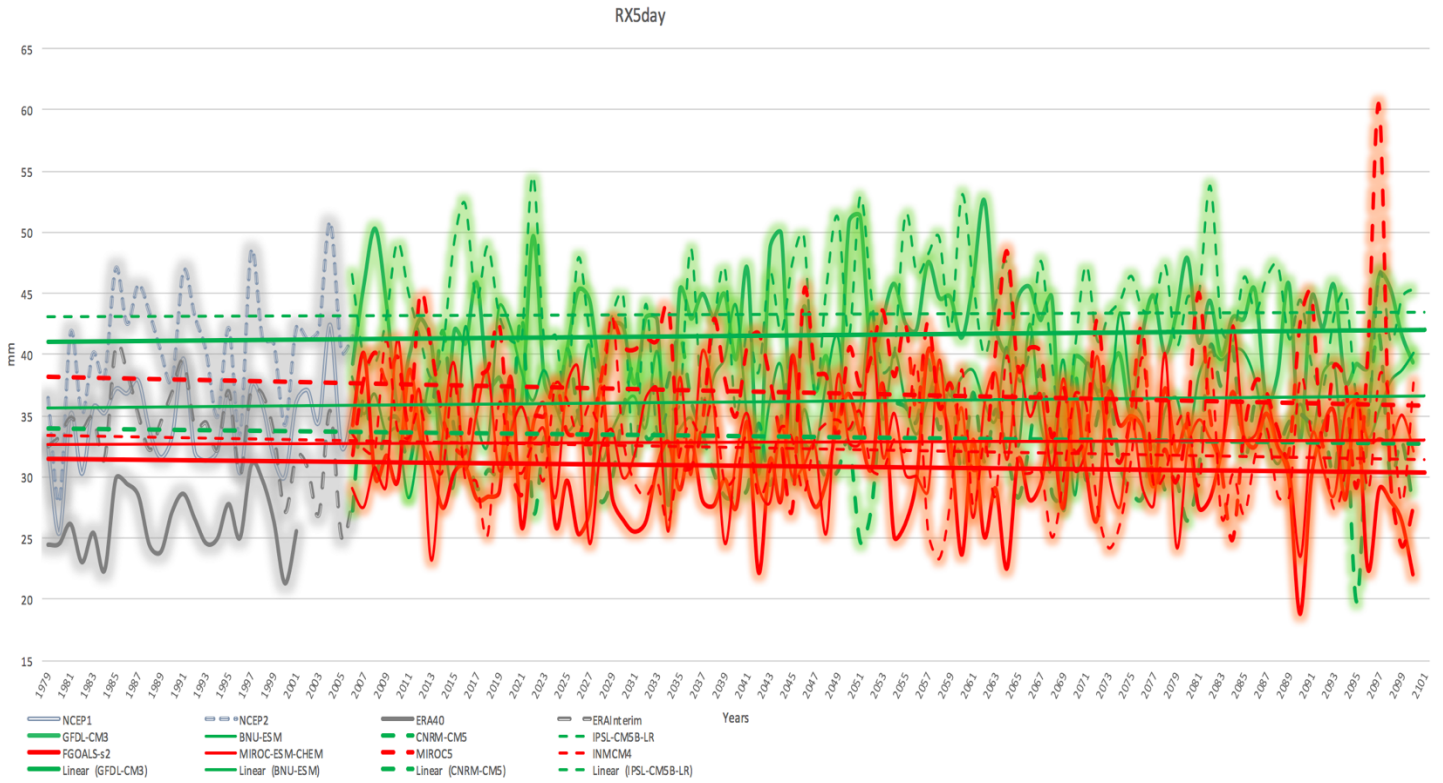


**Figure 3:** Future projections of the “best” and “worst” GCMs for Rx5day extreme index. The gray lines represent the four historical observation-based reanalyses. Green lines show the five lowest (“best”) percentage biases, while the red lines represent the five highest/ (“worst”) percentage biases. Trend lines are included for each of the GCMs projections.

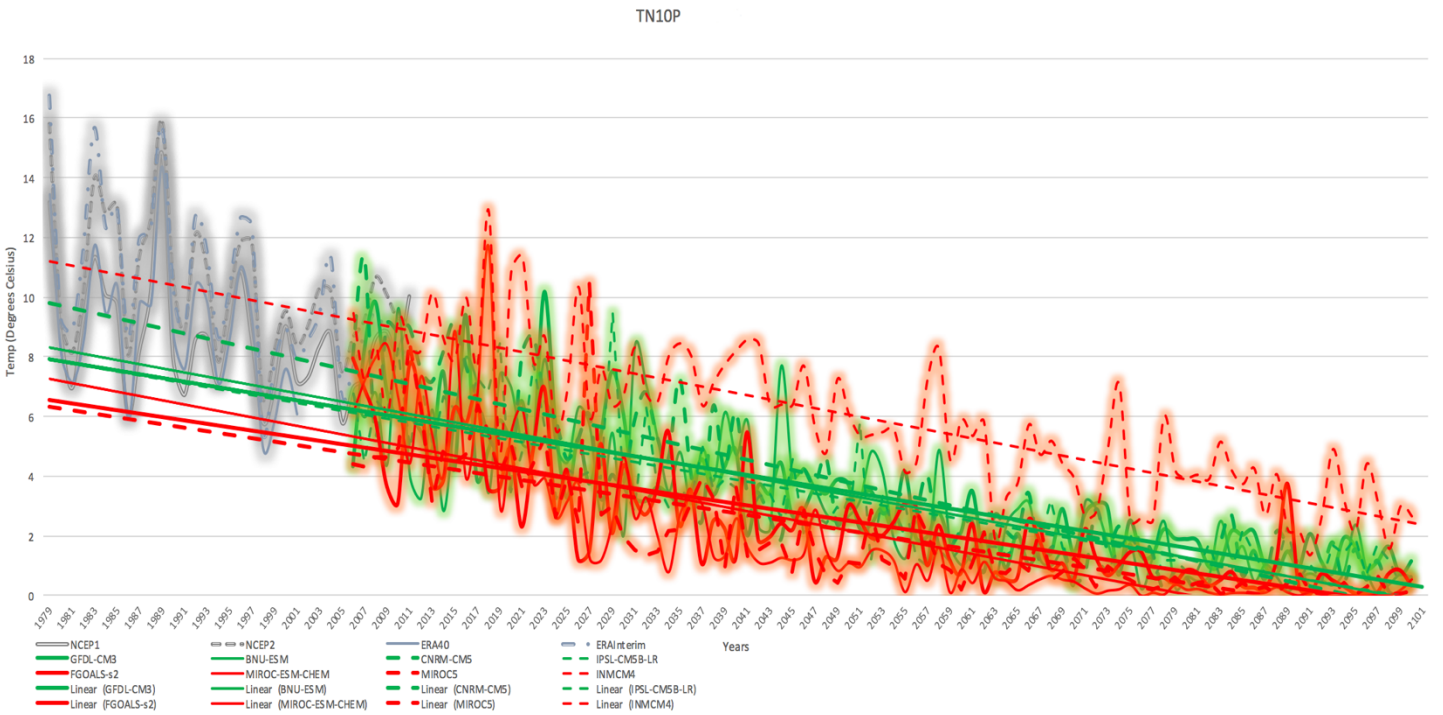


**Figure 4:** Same as Figure 3 but for TN10p.

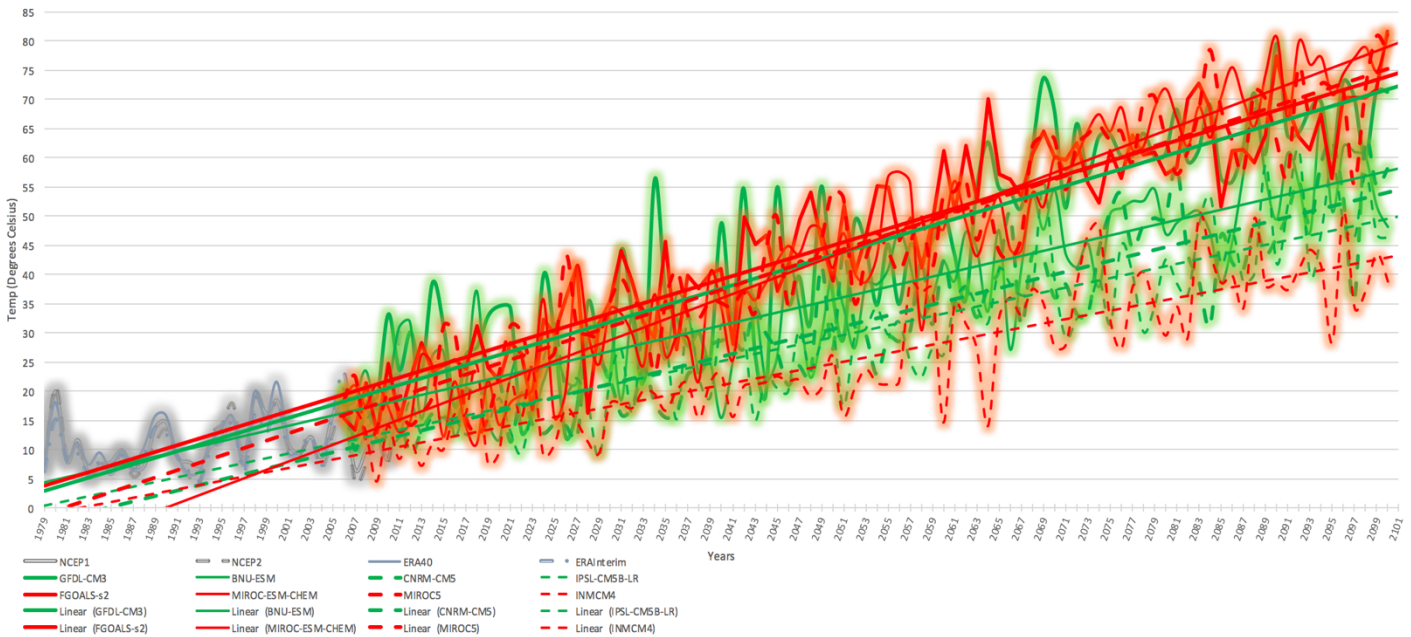


**Figure 5:** Same as Figure 3 but for TX90p.

EraInterim tended to be within a low to medium range of bias, while each of the other reanalyses show noticeably higher biases when used as the “ground truth” depending on the region and/or extreme. Each observation-based reanalysis simulates the past differently. When comparing the percentage bias against each reanalysis it is clear that there is not one universal “best”. The “best” and “worst” varies depending largely on the extreme and region. This suggests that in order to get the most accurate depiction of the past multiple observation-based reanalyses must be compared.

Tables 7,8, and 9 show the ranking of GCMs per season as well as across all the seasons for each sub-region. The top and bottom five per region for each seasonal group are compiled in Table 10. The best and worst performing models varied in relation to region and season. Models from the same institution tended to contain similar biases. For example, many of the MIROC GCMs had consistently higher biases.

Future projections of RX5day showed that most of the best models predicted a larger maximum 5-day precipitation than the worst models did (Figure 3). Better models also

had a generally higher TN10p than the worse models (Figure 4) - although, one model (INMCM4) is consistently higher than the closely grouped best models. The best TX90p model projections tended to be lower than those of the worst, but once again one model (INMCM4) was consistently lower than the best model projections (Figure 5).

For this study we were only able to thoroughly analyze a few of the “best” and “worst” models in order to project into the future. More work is needed in this area before we can make any robust conclusions regarding a secular difference between the “best” and “worst” models.

#### 4.SUMMARY

For the purpose of this study, the south-central region of the U.S. was divided into three sub-regions: west-central, south-central, and east-central. We used output from 30 of the CMIP5 GCMs historical simulations and future projections of emissions scenarios RCP2.6, 4.5 and 8.5. Using data from four observation-based reanalyses as a means for comparison, a NCL program was used to calculate the GCMs historical simulation percentage bias

for each month in the available years. These percentage biases were averaged per season and plotted as a bias/portrait diagram, which acts as a visually appealing and comprehensive way to convey differences in biases across all the GCMs and extreme indices per region. Absolute values for the biases were used to generate an average percentage bias of each observation-based reanalysis for all of the GCMs per extreme. This allowed us to compare the bias associated with each observation-based reanalysis per extreme, as well as averaged across each extreme. We used a similar method in order to determine the five GCMs with the lowest and highest percentage bias, (the “best” and “worst” performing models respectively) and average the GCMs bias percentages per each season and overall.

TNn, as well as several other extremes show noticeably higher percentage bias in each sub-region. This is especially apparent in transition seasons (spring and fall). Previous studies have suggested that climate and weather extremes are more likely during transitions seasons such as these (Alexander et al. 2006; Donat et al. 2013; Nicholas 2014). In the case of TNn however this was primarily due to the mean season value in certain reanalyses falling close to 0°C, which occurred most often during these seasons. When seasonally averaged, this number may tend to fall further from the 0-degree Celsius threshold, causing the percentage bias to appear larger. Further research would be required in order to test the validity of this theory.

In the west-central region increased bias is present for precipitation extremes (Rx1day and Rx5day) during the summer as well as the transition seasons. This suggests that other factors may be affecting this region. The west-central has topography ranging from high mountain peaks to low valleys.

The Rocky Mountains as well as various other mountain ranges extend into this area. The most abundant precipitation in the region occurs between May and September, associated with the North American Monsoon (NAM; NOAA 2004). This period of time correlates with the timing of the higher heavy rainfall biases, suggesting that the simulation of NAM departs in frequency and/or magnitude compared with reanalyses. The inability of models to accurately simulate the topography of the region and/or NAM and its effect on precipitation and temperature are two possible factor contributing to higher biases amongst TNn for all regions (particularly the south- and west-central domains) and precipitation extremes in the west-central domain. The particularly high TNn biases are seen across all three regions but particularly in the south- and west-central domain. This may be related to any number of the previous factors. Another possible explanation for this is that the eastern sub-domain of this region may tend to be warmer.

Failing to normalize the percentage biases was a limit for this study. The observation-based reanalyses large bias spread (with biases getting as high as 539%), is attributed to values within the observation-based data that are close to 0 when averaged seasonally. Compared model values would therefore create a very large percentage bias if they were not also close to 0. This can be resolved by normalizing the data.

Research on GCM biases in specific regions helps scientists better understand how models perform in these areas. The use of several observation-based reanalysis reaffirms that users must be careful not to assume that these are entirely accurate depictions of past climate. Future projections show that there is a possibility of

different magnitudes of the best and worst model trends. This could be useful for better constraining the magnitude of possible future climate change for this region.

## 5. ACKNOWLEDGEMENTS

Thank you to Dr. Esther Mullens, who developed the NCL codes used in this research.

This material is based upon work supported by the National Science Foundation under Grant No. AGS-1560419.

## 6. REFERENCES

Alexander, L.V., and Coauthors, 2006: Global Observed Changes in Daily Climate Extremes of Temperature and Precipitation. *J. of Geophysical Research*, **111**, doi:10.1029/2005JD006290

Donat, M.G. and Coauthors, 2013: Updated Analyses of Temperature and Precipitation Extreme Indices Since the Beginning of the Twentieth Century: The HadEX2 Dataset. *J. of Geophysical Research: Atmospheres*, **118**, 2098-2118. doi:10.1002/jgrd.50150.

Kunkel, K.E, L.E. Stevens, S.E. Stevens, L. Sun, E. Janssen, D. Wuebbles, M.C. Kruk, D.P. Thomas, M. Shulski, N. Umphlett, K. Hubbard, K. Robbins, L. Romolo, A. Akyuz, T. Pathak, T. Bergantino, and J.G. Dobson, 2013: Regional Climate Trends and Scenarios for the U.S. National Climate Assessment. *Climate of the U.S. Great Plains, NOAA Technical Report NESDIS*, 142-4, 82.

NOAA, 2004: The North American Monsoon. National Weather Service Forecast Office: Tucson, AZ, Accessed 1 October 2016. [Available online at

[http://www.wrh.noaa.gov/twc/monsoon/monsoon\\_NA.php](http://www.wrh.noaa.gov/twc/monsoon/monsoon_NA.php)]

Shafer, M., D. Ojima, J. M. Antle, D. Kluck, R. A. McPherson, S. Petersen, B. Scanlon, and K. Sherman, J. M. Melillo, Terese (T.C.) Richmond, and G. W. Yohe, Eds., 2014: Climate Change Impacts in the United States. The Third National Climate Assessment, *U.S. Global Change Research Program*, 441-461. doi:10.7930/J0D798BC.

Sillmann, J., V.V. Kharin, X. Zhang, F.W. Zwiers, D. Bronaugh, 2013: Climate Extremes Indices in the CMIP5 Multimodel Ensemble: Part 1. Model Evaluation in the Present Climate. *J. of Geophysical Research: Atmospheres*, **118**, 1716-1733, doi:10.1002/jgrd.50203.